INTL JOURNAL OF ELECTRONICS AND TELECOMMUNICATIONS, 2026, VOL. 72, NO. 1, PP. 1-8
Manuscript received October 15, 2025; revised January, 2026. doi: 10.24425/ijet.2026.157900

Substrate size impact on the radiation pattern of a sub-THz printed antenna

Yevhen Yashchyshyn, and Peter Tokarsky

***Abstract*—In this paper, we study the effect of the transverse dimensions of a "thick" substrate on the printed antenna radiation properties in the sub-THz range. A four-element series-fed dipole array operating at 100-116 GHz is chosen as a test antenna. It is printed on a rectangular grounded aluminum oxide substrate (99.5% Alumina) with a thickness of 0.05 mm, 0.1 mm, or 0.2 mm, in which only the fundamental mode of the surface wave can exist. The studies used the full-wave electromagnetic simulation method with Altair FEKO 2022 software. It is shown that pulsations can appear in the main beam of the antenna on atruncated substrate, the frequency of which increases proportionally to the width of the substrate, and the amplitude grows with increasing its thickness. With an increase in the substrate size, quasi-periodic variations in the antenna normal-side directivity and gain are also observed, the period of which is equal to two surface wavelengths. The antenna radiation efficiency weakly depends on the substrate width, but increases noticeably with its thickening. It is shown that using a metasurface that significantly weakens the surface wave is an effective means of reducing the substrate edges' effect on the antenna characteristics.**

***Keywords*—Printed antenna; thick substrate; surface wave; metasurface; radiation pattern; antenna directivity**

I. Introduction

IT is expected that the development of sub-THz (0.1-0.3)10^{12} Hz and THz (0.3-10) 10^{12} Hz ranges will significantly expand the possibilities of technical use of electromagnetic waves, in particular, significantly increase the data transfer rate in telecommunication systems [1], increase the capacity of communication channels [2], increase the resolution in radar [3], [4], improve the quality of non-invasive diagnostics in biomedical applications [5], etc.

Essential components of THz technology are antennas. At sub-THz, various types of antennas are used, including traditional horn, mirror, lens, microstrip, leaky-wave, and slot-waveguide antennas [6], taken from the microwave range, as well as new dielectric antennas [7], [8], chip antennas, crystal antennas [9], etc.

Printed microstrip antennas [10], known for their apparent advantages such as lightweight, low-profile design, affordability, seamless integration with other devices, and efficient, low-cost mass production, can also be used at THz [11]. One of the main factors complicating the use of microstrip antennas in the sub-THz range is that substrates have a large electrical thickness, on which intense surface waves (SWs) are excited. They can significantly degrade the antenna performance, particularly reducing the radiation efficiency and narrowing the bandwidth [12]. In addition, SW reflections from the substrate edges can also significantly affect the printed antenna radiation pattern (RP), which is expressed in distortion of its shape, reduction of directivity, growth of side lobes, etc.

Not many works are devoted to considering the influence of the substrate size on the RP of printed antennas, which use different approaches to solving this problem. The first works [13]-[15], published in the 80th - 90th of the last century, proposed approximate solutions based on the geometric (GTD) or physical (PTD) theory of diffraction to solve this problem. In parallel with them, experimental studies of the parameters of finite-size microstrip antennas were performed [16], [17], [18], where special attention was paid to their directional properties. A significant step forward in the development of these studies was the appearance of works [19]-[21], in which rigorous solutions to the problem were proposed using the integral equation (IE) method and the finite difference time domain (FDTD) method. Further studies of printed antennas on finite substrates were performed using computer electromagnetic modeling [22]-[24] using well-known software. Microstrip rectangular patch antennas were the objects of study in the above works, except [13], where the

TABLE I
COMPARISON OF SUBSTRATE PARAMETERS IN THE REFERENCES

Ref.	f (GHz)	h (mm)	ε_r	λ_d (mm)	h_d	Method or Software
[13]	2.295	3.175	2.55	81.86	0.039	GTD
[14]	5.0	2.0	4.0	30.0	0.067	PTD
[15]	2.35	3.175	2.55	81.86	0.039	GTD
[16]	6.8	3.175	2.33	28.90	0.11	Exper.
[17]	5.66	1.27	10.2	16.6	0.077	Exper.
[18]	1.050	1.524	3.25	187.6	0.008	Exper.
[19]	4.97	0.8	4.34	28.97	0.028	IE
[20]	1.88	0.7874	2.33	100.9	0.008	IE
[21]	6.458	3.0	2.32	30.50	0.098	FDTD
[22]	1.8	3.175	2.5	105.4	0.03	HFSS
[23]	3	1.27	10.2	31.31	0.041	WIPL-D
[24]	2	1.27	10.2	46.97	0.027	CST MS

This work was supported with basic funding from the Institute of Radioelectronics and Multimedia Technology, Warsaw University of Technology.

The article was a preprint on Research Square (2025), https://doi.org/10.21203/rs.3.rs-5670493/v1

Yevhen Yashchyshyn is with Institute of Radioelectronics and Multimedia Technology, Warsaw University of Technology, Poland (e-mail: Yevhen.yashchyshyn@pw.edu.pl).

Peter Tokarsky is with Institute of Radio Astronomy, National Academy of Sciences of Ukraine, Ukraine (e-mail: p.l.tokarsky@gmail.com).

© The Author(s). This is an open-access article distributed under the terms of the Creative Commons Attribution License (CC BY 4.0, https://creativecommons.org/licenses/by/4.0/), which permits use, distribution, and reproduction in any medium, provided that the Article is properly cited.

field source was a linear magnetic current thread lying on a grounded substrate.

To facilitate comparison of the results of the referenced works, Table I shows the thickness h of the dielectric substrate used in each of them, its relative permittivity ε_r, and the maximum frequency $f_{\max}$ at which the studies were performed, as well as the method and/or software employed These data made it possible to calculate the wavelength in the substrate dielectric $\lambda_d = c/(f_{\max}\sqrt{\varepsilon_r})$, where c is the speed of light in free space, and the electrical thickness of the substrate $h_d = h/\lambda_d$. Each of the listed values is assigned a separate column in Table 1.

The studies described in referenced papers show that the RP of patch antennas on finite substrates differs significantly from the RP of similar antennas on infinite substrates. These differences mainly consist of the antenna's back radiation and the appearance of some waviness on its RP main lobe in the E plane, with PR shape depending on the transverse dimensions and substrate thickness.

In the literature, it is common to rank the substrates of printed antennas by their electrical thickness as thin, moderate, and thick. Let us briefly consider how it looks in numerical terms.

According to [25], [26], the substrate is thin if its thickness lies within the range $0 < h \le h_{\max}$, where

$$h_{\max} = \frac{0.3c}{2\pi f_{\max}\sqrt{\varepsilon_r}} \approx 0.048\lambda_d \qquad (1)$$

The authors of [25] believe that the losses in antennas associated with the surface wave in such substrates are negligibly small. We used the technique given in [27] to estimate the level of these losses. We found that the power spent on creating a surface wave in a microstrip antenna with the substrate of thickness $h_{\max}$ is indeed relatively small and is approximately 1/6 of the input power of the antenna.

Substrates of moderate electrical thickness occupy an intermediate position between thin and thick ones. The lower limit of their thickness coincides with $h_{\max}$, while its upper limit is not clearly defined anywhere. However, we can suppose that it is approximately equal to $2h_{\max}$, based on the works in which their authors describe the substrate height as moderately [17], [28], [29], etc. In this case, the moderate substrate thickness will be limited by the following inequality: $h_{\max} < h \le 2h_{\max}$. Therewith, the antenna power spent on creating a surface wave in a substrate $2h_{\max}$ thick will be approximately one-third of the antenna input power. It also follows that substrates of thickness $h > 2h_{\max}$ can be considered electrically thick.

Returning to Table I, we can see that most of the presented works here consider antennas on thin substrates, two works, [14] and [17], on moderate substrates, and two more on substrates that are formally classified as thick, but not much thicker than the moderate ones. Therefore, the results of these studies cannot, unfortunately, be a priori extended to the sub-THz range, where seemingly thin dielectric substrates turn out to be electrically thick, reaching $(4-5)h_{\max}$ [30].

This work aims to evaluate the influence of the thick substrate dimensions on the directional properties of printed antennas in the sub-THz range and to study the possibility of reducing it using metasurface elements.

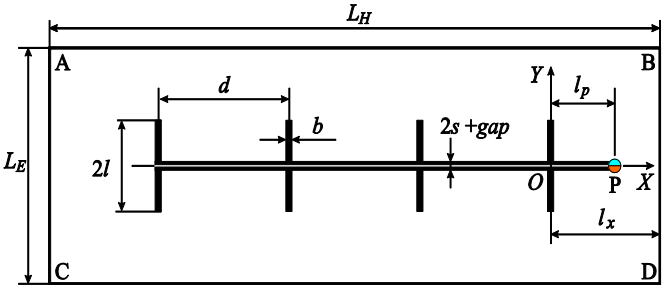

Fig. 1. Dipole array layout: $2l$ = 0.7 mm, b = 0.05 mm, s = 0.02 mm, gap = 0.01 mm, d = 1.2 mm, l_p = 0.56 mm, l_x = 1.0 mm, L_H = 5.6 mm.

II. Design of the Antenna Under Study

A dipole antenna array with a series feed (Figure 1) was selected for the study. It was printed on a rectangular grounded substrate made of aluminum oxide (99.5% Alumina), which has a sufficiently high permittivity ($\varepsilon_r = 9.75$) and low losses ($\tan\delta = 0.0003$). This material is promising for use in the mm and THz ranges [31]-[34] and has already been repeatedly used in the design of millimeter-wave antennas [35]-[38]. The substrate thickness h was chosen from the condition that guarantees the existence of only the SW fundamental mode TM_0, while all other modes would be beyond the cutoff threshold [25]:

$$h < \frac{c}{4 f_{\max}\sqrt{\varepsilon_r - 1}} \qquad (2)$$

It follows that the thickness of the substrate with a given ε_r should be $h < 0.218$ mm in the range of interest to us, 100-116 GHz. Based on this, we selected three substrate options for our studies: 0.05 mm, 0.1 mm, and 0.2 mm thick. The electrical thicknesses h_d of these substrates are equal to 0.060, 0.121, and 0.242, respectively, i.e., the first should be considered moderate, and the other two should be thick.

Below, for the convenience of presentation, we will call the dipole antenna array under study an antenna.

First, let us consider the antenna located on a grounded infinite substrate, the characteristics of which are not affected by the edges. SWs excited by the antenna run away to infinity along the Y-axis on the substrate-air interface, carrying with them part of the power.

The wavelength of the SW can be found in the following relation [26]

$$\lambda_{TM0} = \lambda_0 / \sqrt{\varepsilon_r - \xi^2} \qquad (3)$$

where λ_0 is the wavelength in free space, ξ is the root of the dispersion equation

$$\varepsilon_r\sqrt{\varepsilon_r - \xi^2 - 1} - \xi\tan(k_0 h\xi) = 0 \qquad (4)$$

The above relationships determine the basic parameters of the substrate that we will need to solve the problem.

The studies announced in the objectives of this work were carried out using the full-wave electromagnetic modeling method using the well-known commercial software Altair

Feko 2022 [39], which has proven its high efficiency in the analysis and design of a broad class of microwave and sub-THz antennas [40], [41].

The models of the considered antennas were constructed assuming all conductors are perfect.

III. Results and Discussion

A. Antenna on an Infinite Substrate

First, we will consider the antenna characteristics under study on an infinite grounded substrate, which we will need later for comparison.

Fig. 2 depicts the 2D distribution of the Y-component of the Poynting vector of the SW excited by the antenna, obtained as a result of the simulation. Here, the thick black lines show the assumed boundaries of the substrate along the X-axis, which it will have after truncation. It follows from the Fig.2 that the SW propagates along the Y axis and in the considered region has the form of a fairly narrow beam, the amplitude of which has a maximum at $X \approx -2$ mm, and at the future boundaries of the substrate (at $Y \le 6$ mm) it drops by about 10 dB.

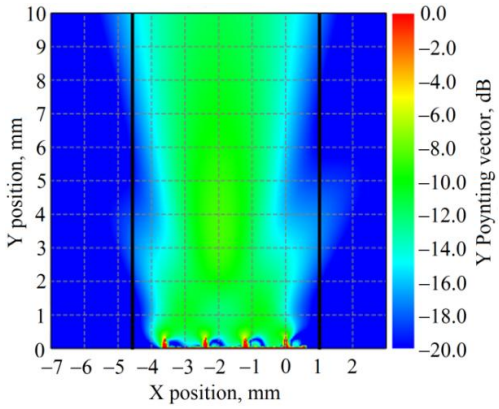

Fig. 2. Distribution of the Poynting vector Y-component at the substrate surface.

Fig. 3 shows the dependence of the ratio $\Lambda = \lambda_{TM0}/\lambda_0$ on the substrate thickness at the middle and extreme frequencies of the considered range of 108-116 GHz.

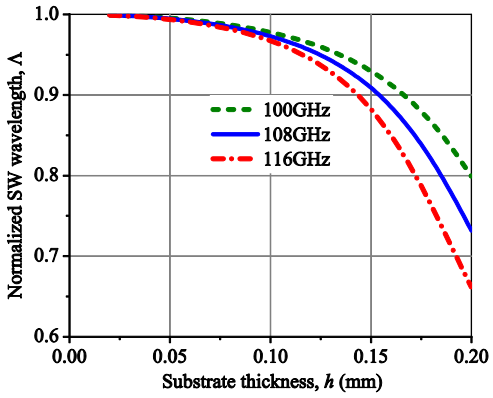

Fig. 3. Normalized SW wavelength Λ vs. substrate thickness.

This evinces that when the substrate thickness $h < h_{\max}$ (2), the SW wavelength is almost the same as λ_0, but with growing h, it falls at an increasing rate, which becomes even more with increasing frequency.

Fig. 4 demonstrates the antenna RPs on an infinite substrate with thicknesses $h = 0.05$ mm, 0.1 mm, and 0.2 mm at a frequency of 108 GHz. Here, it can be clearly seen that the shown antenna RP in the H plane completely corresponds to the RP of a 4-element uniform array, the half-power width of its main beam is 30° and remains almost unchanged with increasing h, and the side lobe level does not exceed –13.2 dB. In the E plane, the RP has no side lobes, and its half-power width decreases with increasing h: from 160° (at $h = 0.05$ mm) to 138° (at $h = 0.10$ mm), and 126° (at $h = 0.20$ mm).

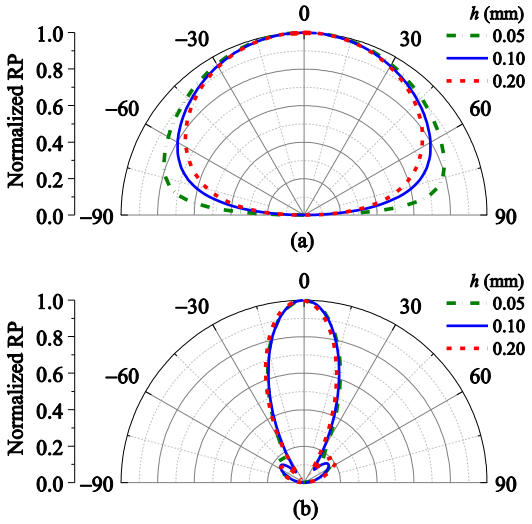

Fig. 4. The antenna RPs on infinity substrates at 108 GHz: (a) E plane, (b) H plane.

This narrowing of the RP causes a monotonic increase in the antenna directivity D: 9.4 dB, 10.1 dB, and 11.4 dB for $h = 0.05$ mm, 0.1 mm, and 0.2 mm, respectively. At the same time, the dependence of the antenna gain G on h turns out to be non-monotonic: 7.2 dB, 8.0 dB, and 7.5 dB the same thicknesses h. We can easily explain this effect as follows.

The power P_{in} consumed by the antenna from the generator is spent on the radiation of spatial waves into free space P_{rad}, on the excitation of a surface wave P_{sw}, and losses in the dielectric P_σ. Let us consider the dependences of these powers on the substrate thickness h, presented in Fig. 5, in normalized form: $e_{rad} = P_{rad}/P_{in}$, $p_{sw} = P_{sw}/P_{in}$, and $p_\sigma = P_\sigma/P_{in}$.

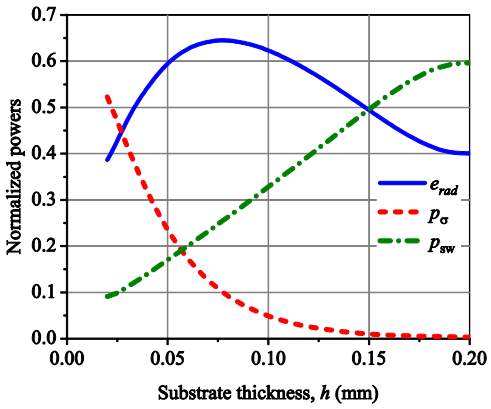

Fig. 5. The antenna power budget at 108 GHz.

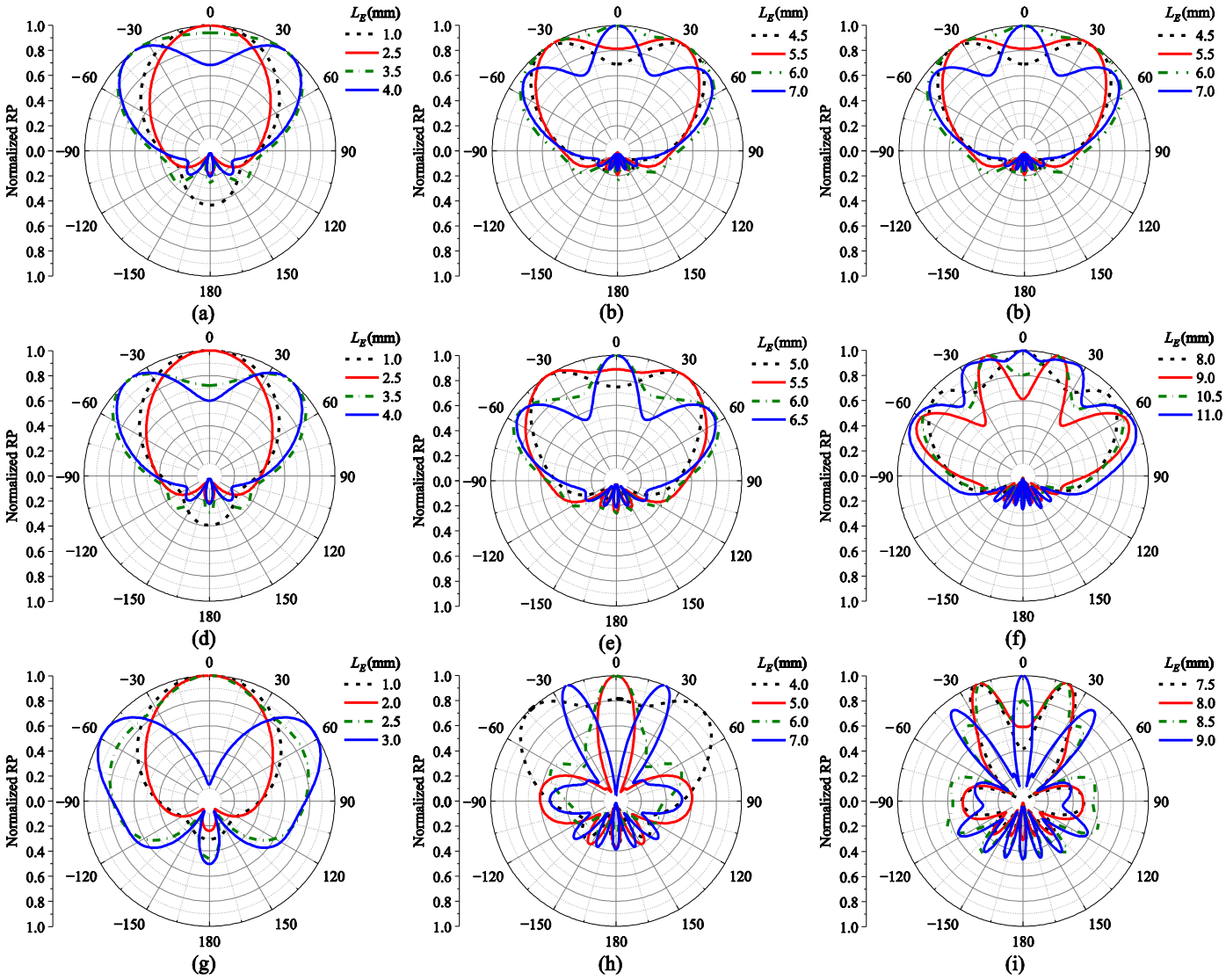

Fig. 6. The antenna normalized RP in the E plane at 108 GHz for different substrate wide L_E and thickness h.

As can be seen from the Fig. 5, with decreasing substrate thickness, the power p_{sw} of the surface wave decreases; however, at the time the power of losses in the dielectric p_σ increases. As a result, the antenna radiation efficiency e_{rad} has a maximum of 0.645 at h=0.077 mm, which causes non-monotonic behavior of the antenna gain G since it is the product $G = e_{rad} D$.

B. Antenna on a truncated Substrate

Now let's consider an antenna on a substrate of finite dimensions (Fig. 1). SWs propagate along the Y axis in opposite directions and, reaching the substrate edges AB and CD, diffract on them, creating an additional radiation field. This field interferes with the main far field of the antenna and reshapes its RP. The AC and BD substrate edges are practically not excited in this case since they are not an obstacle to the propagation of the SW TM_0 mode in the Y-axis direction, and the amplitude of the SW Poynting vector X-component is approximately 10 dB less than its Y-component (Fig. 2). In this regard, we can consider the antenna RP depending on the substrate width L_E only, with its length $L_H = 5.6$ mm fixed.

Simulation results of the antenna evidenced that its RP in the H plane in the upper half-space does not depend on the substrate width L_E and is almost the same as the antenna RP with an infinite substrate, shown in Fig. 4(b). On the contrary, the antenna RP in the E plane depends quite strongly on L_E. Fig. 6 demonstrates how its shape changes with an increase in L_E from 1 mm to 12 mm for different thicknesses $h = 0.05$ mm (Figs. 6(a), 6(b), and 6(c)), 0.1 mm (Figs. 6(d), 6(e), and 6(f)), and 0.2 mm (Figs. 6(g), 6(h), and 6(i)).

We can come to the following conclusions after analyzing the antenna RPs in the E plane:

1. At the substrate width of less than one SW wavelength ($\lesssim$2 mm), the antenna RP has a bulb-shaped main beam with a maximum in the direction of the antenna plane normal.

2. When $L_E > \lambda_{TM0}$, pulsations are superposed on the antenna RP, the period of which decreases with increasing L_E, and the amplitude increases with increasing substrate thickness h.

3. When the substrate thickness h is not very thick (from 0.05 mm to 0.1 mm), the range of the RP pulsations is approximately 2 dB to 3 dB, however, when h reaches 0.2 mm, the main beam of the RP in fact splits into several lobes, the number and directions of which depend on the substrate width L_E.

4. The antenna RP contains back lobes, whose number increases with the substrate width L_E, and their level grows approximately from –25 dB to –5 dB with substrate thickening h from 0.05 mm to 0.2 mm.

There is no doubt that the variations in the antenna RP, visible in Fig. 6, should be reflected in its directivity D and gain G. Fig. 7 reveals the dependence of the directivity D of this antenna in the normal direction on the substrate width, which is normalized to the SW wavelength $l_E = L_E/\lambda_{TM0}$.

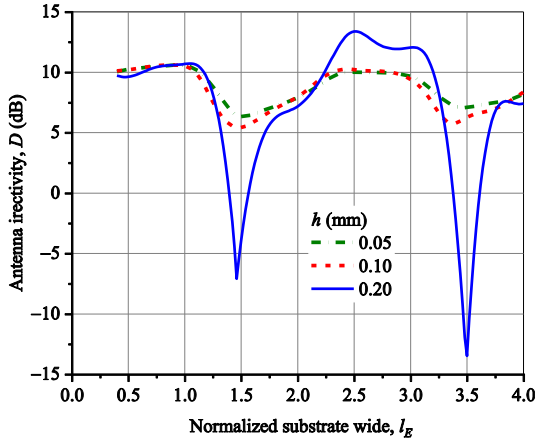

Fig. 7. The antenna directivity at 108 GHz for different substrate thickness, h=0.05 mm, 0.1 mm and 0.2 mm.

The positions of the maxima and minima of all three curves practically coincide, but the values of D at these points differ significantly. If the curves of antenna directivity on substrates with $h = 0.05$ mm and $h = 0.10$ mm vary within (5...9) dB and (5...10) dB, respectively, then at $h = 0.20$ mm, their variation limits expand to (–13...13) dB.

It is natural to assume that the extremes of these curves are caused by the in-phase and out-of-phase addition of the antenna's intrinsic field $\vec{E}_a$ and the edges diffracted field $\vec{E}_d$. To check this assumption, we split the far field $\vec{E}$ of the antenna on the truncated substrate into two components $\vec{E} = \vec{E}_a + \vec{E}_d$.

Fig. 8 depicts the RPs $f(\theta)$ in the E plane of the antenna on substrates with a thickness of $h = 0.20$ mm and a width of $l_E = 0.5$ (Fig. 8(a)), 1.5 (Fig. 8(b)), 2.5 (Fig. 8(c)), and 3.5 (Fig. 8(d)), as well as their components $f_a(\theta)$ and $f_d(\theta)$, all normalized to the field $\vec{E}_a$ in the normal direction: $f(\theta) = E(\theta)/E_a(0)$, $f_a(\theta) = E_a(\theta)/E_a(0)$, and $f_d(\theta) = E_d(\theta)/E_a(0)$. The indicated values of l_E were chosen because, for them the field $\vec{E}_d$ was strictly in-phase or out-of-phase with the field $\vec{E}_a$ in the normal direction.

It follows from Fig. 8 that when the substrate width $l_E = 0.5$ (Fig. 8(a)), the surface waves create a field $\vec{E}_d$ on the substrate edges, which is in phase with $\vec{E}_a$ in the normal direction, and their ratio is $f_d(0) = 0.52 f_a(0)$. If the substrate is expanded to $l_E = 1.5$, the surface waves run an additional $0.5\lambda_{TM0}$ (Fig. 8(b)) and the field $\vec{E}_d$ becomes antiphase to the field $\vec{E}_a$ with their ratio $f_d(0) = -0.87 f_a(0)$. With further expansion of the substrate, the situation is repeated cyclically. When $l_E = 2.5$ (Fig. 8(c)), the surface waves run another $0.5\lambda_{TM0}$ and again create a field $\vec{E}_d$, in phase with $\vec{E}_a$ at $f_d(0) = 0.87 f_a(0)$, and finally, when $l_E = 3.5$, the phase of $\vec{E}_d$ more again changes to the opposite, and its amplitude is practically equal to the amplitude of $\vec{E}_a$, $f_d(0) = -0.98 f_a(0)$. It can assume that with a further increase in the substrate width, the situation will be repeated in a similar way.

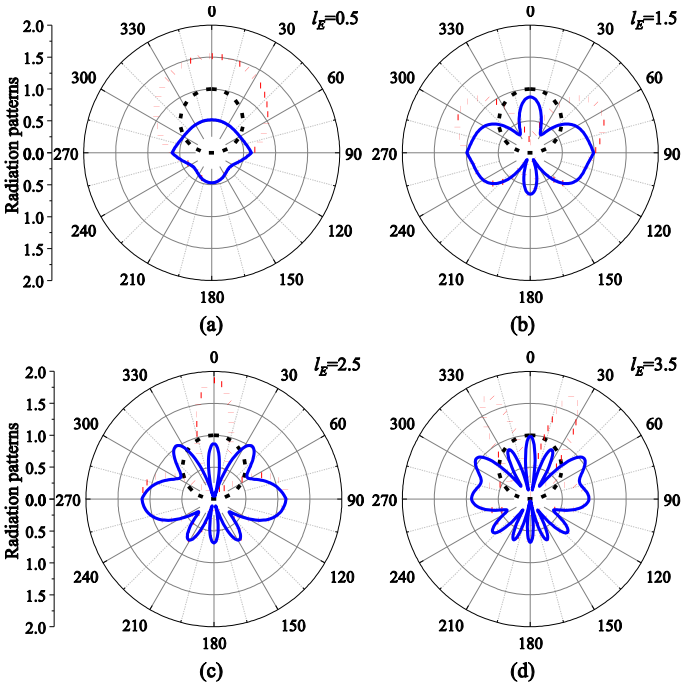

Fig. 8. Decomposition of the antenna far field on the truncated substrate of 0.2 mm thickness and different widths: dotted line – total far field of the truncated antenna; dashed line – the antenna far field on infinity substrate; solid line – the far field due to substrate edges

Now let us consider how the antenna radiation efficiency behaves. Fig. 9 shows its dependence on the normalized substrate width l_E for the same thicknesses $h = 0.05$ mm, 0.1 mm, and 0.2 mm.

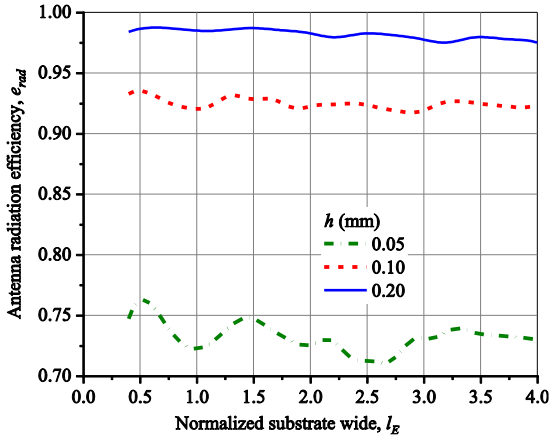

Fig. 9. The antenna radiation efficiency e_{rad} at 108 GHz for different truncated substrate thickness h=0.05 mm, 0.1 mm and 0.2 mm.

It can be seen in Fig. 9 that the antenna radiation efficiency is almost independent of l_E, if we do not take into account its small variations visible in the graphs. Its average values are 0.732, 0.925, 0.981 with deviations of no more than 0.03, 0.01, 0.006 for h=0.05 mm, 0.10 mm, and 0.20 mm, respectively. With the increasing truncated substrate thickness, the antenna radiation efficiency improves due to reduced losses in the dielectric (Fig. 5) that remained the only ones here. Thus, an antenna on the 0.2 mm thick substrate is the most attractive for antenna manufacturing in terms of its radiation efficiency that is very close to 100%. On the other hand, the strong dependence of the RP of such an antenna on the substrate width makes it difficult to choose its optimal size based on other design considerations. Let us show how this undesirable dependence can be reduced by using metasurface (MS) elements.

C. *Antenna with MS Elements*

In [41] it is shown that the use of MS elements in the form of quad split rings QSR (Fig. 10) in printed antennas allows changing the positive surface reactance of the grounded dielectric layer to negative, which prevents the propagation of SW in the layer and thereby increases the radiation efficiency of these antennas. We will use QSR arrays to reduce the influence of the substrate edges on the antenna RP.

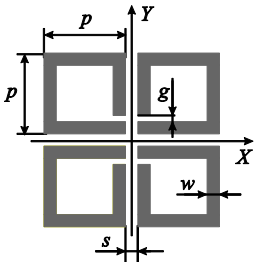

Fig. 10. The metasurface QSR element, p = 165 μm, s = w = 25 μm, g = w/2.

Fig. 11 shows the antenna under study (Fig. 1) with two added arrays of nine QSR elements, the distance between which along the X axis is $d_x = d/2 = 0.6$ mm and along the Y axis is $d_y = 2d = 2.4$ mm.

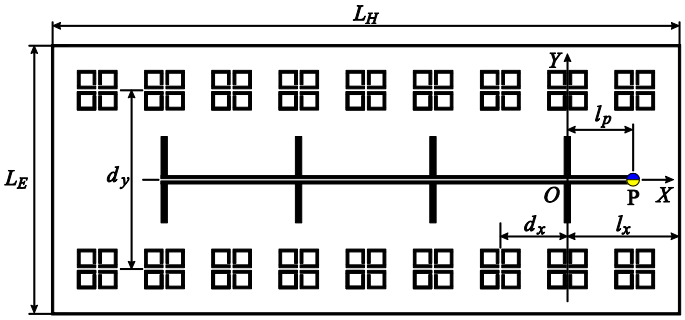

Fig. 11. Layout of the antenna with metasurface QSR elements.

Let us consider how the added metastructure affected the power of the SW in the antenna. Fig. 12 shows the Y-component of the SW Poynting vector magnitude on the surface of an infinite substrate with the different thickness vs. the Y at fixed $X = -2$ mm in the coordinate system indicated in Fig. 2. When calculating this graph, it was assumed that the antenna input power is $P_{in} = 15$ mW.

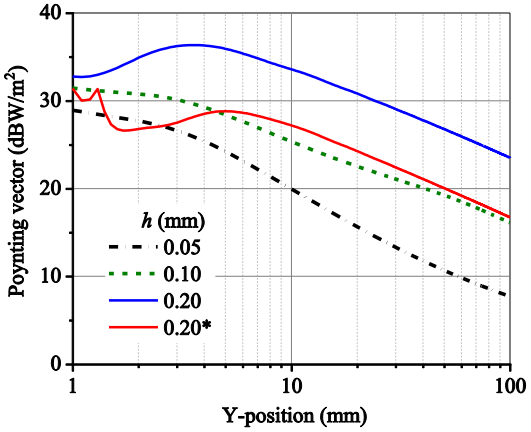

Fig. 12. The Poynting vector magnitude of SW as a function of Y at X=–2 mm;* – with metasurface QSR elements.

It follows from Fig. 12 that the surface wave power flux density decreases by approximately 8 dB (at $Y > 20$ mm) with a halving of the substrate thickness. A similar effect is produced by the proposed metastructure in the antenna under study on a substrate of $h = 0.20$ mm, the use of which decreases the Poynting vector magnitude approximately as much as a halving of h, which should certainly be reflected in the dependence of the antenna RP on the substrate width.

Fig. 13 shows the antenna RP with metasurface elements (Fig. 11) on a 0.2 mm thick substrate for different L_E from 3 mm to 8 mm.

It is evident from it that the antenna RP has no dips in the normal direction with a substrate width of up to $L_E = 7.5$ mm ($l_E = 3.7$), and the first noticeable minimum in the normal direction is observed only at $L_E = 8$ mm ($l_E = 4$), however, it is not as deep as in the RP of the antenna without MS. Its value in the minimum point is 0.5, i.e. the same as in the antenna on the 0.1 mm high substrate (Fig. 6(b)), which was predicted by the graphs in Fig. 13. If it is undesirable for the minimum in the antenna RP to appear precisely at the substrate size $L_E = 8$ mm, it can be shifted by changing the distance between the metaelement arrays d_y (Fig. 11).

There is the antenna RP in Fig. 13(c) with the substrate width $L_E = 8$ mm, in which the distance d_y is reduced to 1.8 mm, is marked with an asterisk. As can be seen from this figure, the minimum in this RP was successfully eliminated, but with $d_y = 1.8$ mm it appears in the antenna RP on the substrate with the width $L_E = 7.4$ mm. Thus, if the antenna has an undesirable minimum in the RP caused by the finite dimensions of the substrate, it can be eliminated using the proposed arrays of metasurface elements by correctly selecting the distance d_y between them.

CONCLUSION

The studies that were performed allowed us to establish the dependence of the directional properties of the printed sub-THz planar antenna on the width and thickness of the substrate. It is shown that the antenna RP in the E plane has one main lobe in the normal direction when the substrate width

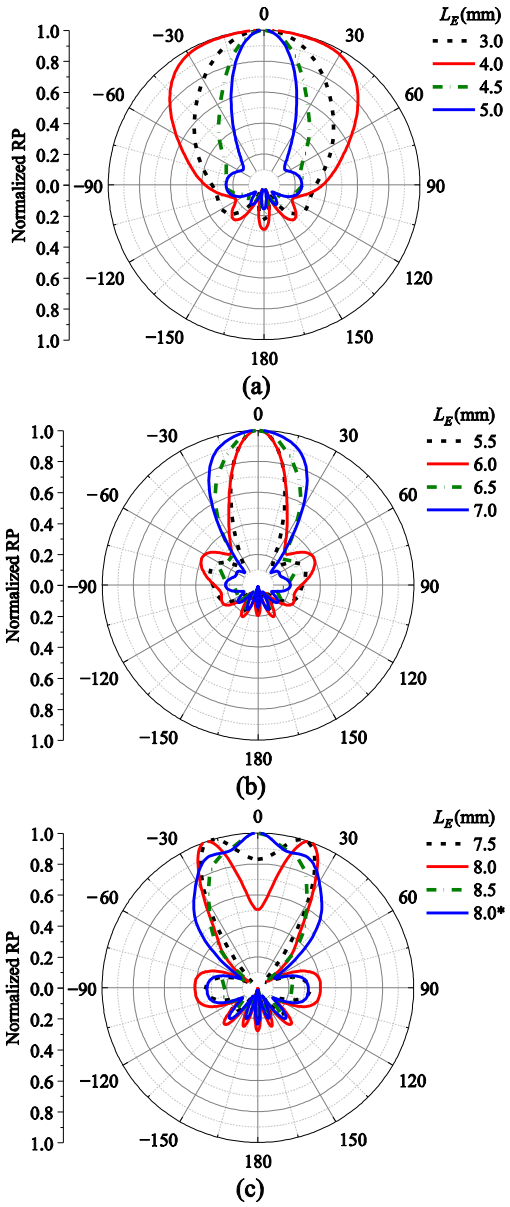

Fig. 11. RPs of the antenna on substrates of different widths using MS with dy=2.4 mm; the exception is the antenna RP marked with *, referred to MS with dy=1.8 mm.

does not exceed one surface wavelength. An increase in the substrate width leads to the appearance of local minima and maxima in the main beam of the antenna RP, the number of which increases with an increase in the substrate width, and the depth of the minima increases with a thickening of the substrate, as a result of which the main beam is divided into several. Changes in the RP lead to quasi-periodic variations in the antenna directivity in the normal direction, the range of which increases with a thickening of the substrate, reaching 26 dB. The peak antenna directivity (as well as its gain) at some values of the substrate width exceeds its level with a short substrate by more than 3 dB. It was also found that the antenna radiation efficiency weakly depends on the substrate width, but noticeably increases with its thickening. All this opens up additional possibilities for antenna optimization by consciously choosing the width and thickness of the substrate. To reduce the influence of the substrate edges on the antenna RP, it is proposed to use arrays of metaelements that significantly weaken the surface wave, which leads to stabilization of the antenna directional properties against the background of a change in the substrate width. The results of this work can help design printed antennas on thick substrates, which will extend their application field into the sub-terahertz range.

REFERENCES

[1] P. Lohan, B. Kantarci, M. A. Ferrag, N. Tihanyi, and Y. Shi, “From 5G to 6G Networks: A Survey on AI-Based Jamming and Interference Detection and Mitigation,” in *IEEE Open Journal of the Communications Society*, vol. 5, pp. 3920-3974, Jun. 2024, https://doi.org/10.1109/OJCOMS.2024.3416808

[2] C. -X. Wang *et al*., “On the Road to 6G: Visions, Requirements, Key Technologies, and Testbeds,” in *IEEE Communications Surveys & Tutorials*, vol. 25, no. 2, pp. 905-974, Secondquarter 2023, https://doi.org/10.1109/COMST.2023.3249835

[3] S. Bruni, M. A. Campo, E. Tolin, and O. Litschke, “Antenna Integration in sub-Terahertz Radar Systems,” in *Proc. 47th Int. Conf. on Infrared, Millimeter and Terahertz Waves (IRMMW-THz)*, Delft, Netherlands, Aug.-Sept. 2022, pp. 1-3, https://doi.org/10.1109/IRMMW-THz50927.2022.9896006.

[4] L. Daniel and M. Gashinova, “Sub-THz Radar Imagery for Automotive Application,” in Proc. *19th European Radar Conference (EuRAD)*, Milan, Italy, Oct. 2022, pp. 261-264, https://doi.org/10.23919/EuRAD54643.2022.9924931

[5] S. K. Koul and·P. Kaurav, *Sub-Terahertz Sensing Technology for Biomedical Applications*, Singapore: Springer Nature Singapore Pte Ltd, 2022, https://doi.org/10.1007/978-981-19-3140-6

[6] M. A. Jamshed, A. Nauman, M. A. B. Abbasi, and S. W. Kim, “Antenna selection and designing for THz applications: Suitability and performance evaluation: A Survey,” *IEEE Access*, vol. 8, pp. 113246-113261, Jun. 2020, https://doi.org/10.1109/ACCESS.2020.3002989

[7] D. F. Filipovic, G. P. Gauthier, S. Raman, and G. M. Rebeiz, “Off axis properties of silicon and quartz dielectric lens antennas,” *IEEE Trans. Antennas Propag.*, vol. 45, no.5, 760-766, May 1997, https://doi.org/10.1109/8.575618

[8] N. Llombart, G. Chattopadhyay, A. Skalare, and I. Mehdi, “Novel terahertz antenna based on a silicon lens fed by a leaky wave enhanced waveguide,” *IEEE Trans. Antennas Propag.*, vol. 59, no. 6, pp. 2160-2168, Jun. 2011, https://doi.org/10.1109/TAP.2011.2143663

[9] J. C. F. Zandboer, G. Federico, U. Johannsen, and A. A. Bart Smolders, “Review on antenna technology developments for sub-THz wireless communication: application, challenges and opportunities,” in *IEEE Open Journal of Antennas and Propagation*, vol. 6, no. 3, pp. 645-663, Jun. 2025, https://doi.org/10.1109/OJAP.2025.3546122

[10] D. Jackson “Microstrip antennas,” in *Antenna Engineering Handbook, 4th Ed.*, J .L. Volakis, Ed. New York, NY, USA: McGraw-Hill, 2007.

[11] M. Zubair, A. Jabbar, F.A. Tahir, J. R. Kazim, M. Rehman, M. Imran, B. Liu, and Q. H. Abbasi, “A high-performance sub-THz planar antenna array for THz sensing and imaging applications,” *Sci. Rep.*, vol. 14, 17030, Jul. 2024, https://doi.org/10.1038/s41598-024-68010-9

[12] D. R. Jackson, S. A. Long, J. T. Williams, and V. B. Davis, “Computer-Aided Design of Rectangular Microstrip Antennas,” in *Advances in Microstrip and Printed Antennas*, Kai Fong Lee and Wei Chen, Ed. New York, NY, USA: John Wiley & Sons, Inc., pp.223-272, 1997.

[13] J. Huang, “The finite ground plane effect on the microstrip antenna radiation patterns,” in *IEEE Trans. Antennas Propag.*, vol. 31, no. 4, pp. 649-653, Jul. 1983, https://doi.org/10.1109/TAP.1983.1143108

[14] A. K. Bhattacharyya, “Effects of ground plane and dielectric truncations on the efficiency of a printed structure,” in *IEEE Trans. Antennas Propag.*, vol. 39, no. 3, pp. 303-308, Mar. 1991, https://doi.org/10.1109/8.76326

[15] V. Volski and G. Vandenbosch, “Radiation pattern of a microstrip antenna located on a finite size ground plane with small vertical wall at the edges,” In *2001 Eleventh International Conference on Antennas and Propagation*, Manchester, UK, 17-20 Apr. 2001; vol. 2, pp. 619-622, https://doi.org/10.1049/cp:20010363

[16] E. Chang, S. Long, and W. Richards, “An experimental investigation of electrically thick rectangular microstrip antennas,” in *IEEE Trans. Antennas Propag.*, vol. 34, no.6, pp. 767-772, Jun. 1986, https://doi.org/10.1109/TAP.1986.1143890

[17] D. Schaubert and K.Yngvesson, “Experimental study of a microstrip array on high permittivity substrate,” in *IEEE Trans. Antennas Propag*., vol. 34, no. 1, pp. 92-97, Jan. 1986, https://doi.org/10.1109/TAP.1986.1143723

[18] M. Sanad, “Microstrip antennas on very small ground planes for portable communication systems,” in *Proc. IEEE Antennas Propag. Soc. Int. Symp. (APSURSI)*, Seattle, WA, USA, 20-24 Jun. 1994; vol. 2, pp. 810-813. https://doi.org/10.1109/APS.1994.407968

[19] S. A. Bokhari, J. R. Mosig, and F. E. Gardiol, “Radiation pattern computation of microstrip antennas on finite size ground planes,” in *IEE Proceedings H (Microw. Antennas Propag.)*, vol. 139, no. 3, pp.278-286, Jun. 1992, https://doi.org/10.1049/ip-h-2.1992.0050

[20] W. Zhou and P. F. Wahid, “Analysis of microstrip antennas on finite ground planes,” *Microwave and optical technology letters*, vol. 15, no. 4, pp. 204-207, Dec. 1997, https://doi.org/10.1002/(SICI)1098-2760(199707)15:4<204::AID-MOP5>3.0.CO;2-J.

[21] S. Chebolu, S. Dey, R. Mittra, and J. Svigelj, “Efficient Modeling of Microstrip Antennas Using the Finite-Difference Time-Domain Method,” in *Advances in Microstrip and Printed Antennas*, Kai Fong Lee and Wei Chen, Ed. New York, NY, USA: John Wiley & Sons, Inc., 1997, pp.515-552.

[22] F. Tavakkol-Hamedani, L. Shafai, and G. Z. Rafi, “The effects of substrate and ground plane size on the performance of finite rectangular microstrip antennas,” in *IEEE Antennas and Propagation Society International Symposium*, San Antonio, TX, USA, 16-21 Jun. 2002; vol. 1, pp. 778-781, https://doi.org/10.1109/APS.2002.1016458

[23] B. Kolundzija and B. Bajic, “Precise modeling of microstrip patch antennas (finite metalization, substrate and ground),” In *Proc. IEEE Antennas Propag. Soc. Int. Symp.*, San Antonio, TX, USA, 16-21 Jun. 2002; vol. 1, pp. 434-437, https://doi.org/10.1109/APS.2002.1018245

[24] T. J. Cho and H. M. Lee, “Front-to-back ratio improvement of a microstrip patch antenna by ground plane edge shaping,” in *2010 Proc. IEEE Antennas Propag. Soc. Int. Symp.*, Toronto, ON, Canada, 11-17 Jul. 2010, pp. 1-4, https://doi.org/10.1109/APS.2010.5561174

[25] R. Garg, P. Bhartia, I. Bahl, and A. Ittipiboom, “*Microstrip Antenna Design Handbook*,” Norwood, MA, USA: Artech House, 2001.

[26] R. Bancroft, *Microstrip and Printed Antenna Design*, 2nd ed.; SciTech Publishing, Inc.: Raleigh, NC, USA, 2009; p. 61.

[27] D. M. Pozar, “Rigorous closed-form expressions for the surface wave loss of printed antennas,” *Electronics Letters*, vol. 26, no. 13, pp. 954-956, Jun. 1990, https://doi.org/10.1049/el:19900622

[28] K. Rambabu, M. Alam, J. Bornemann, and M. A. Stuchly, “Compact wideband dual-polarized microstrip patch antenna,” in *2004 Proc. IEEE Antennas Propag. Soc. Int. Symp.*, Monterey, CA, USA, 20-25 Jun. 2004; vol. 2, pp. 1955-1958, https://doi.org/10.1109/APS.2004.1330587

[29] D. C. Nascimento, P. C. R. Filho, A. F. Tinoco-S, and J. C. da S. Lacava, “Analysis and design of cavity-backed probe-fed hybrid microstrip antennas on FR4 substrate,” in *International Journal of Antennas and Propagation*, vol. 2015, no. 1, 206967, Oct. 2015, https://doi.org/10.1155/2015/206967

[30] H-J. Song, “Packages for terahertz electronics,” in *IEEE Proc.*, vol. 105, no. 6, pp. 1121-1138, June 2017, https://doi.org/10.1109/JPROC.2016.2633547

[31] R. Rodriguez-Cano, S. Perini, and M. T. Lanagan, “Dielectric Characterization of Materials at 5G mm-Wave Frequencies,” in *Proc. 18th Eur. Conf. Antennas Propag. (EuCAP)*, Mar. 2024, Glasgow, UK, https://doi.org/10.23919/EuCAP60739.2024.10501433

[32] P. Palani, R. Behera, A. Andhiwal, K. Singh, and A. V. Nirmal, “Detailed Characterization of Indigenous Alumina Substrates for Thin & Thick Film Hybrid Microcircuits,” in *Proc. 3rd International Conference for Emerging Technology (INCET)*, Belgaum, India, May 2022. https://doi.org/10.1109/INCET54531.2022.9824634

[33] M. Ma, Y. Wang, M. Navarro-Cía, F. Liu, F. Zhang, Z. Liu, Y. Li, S. M. Hanham, and Z. Hao, “The dielectric properties of some ceramic substrate materials at terahertz frequencies,” in *Journal of the European Ceramic Society*, vol. 39, no. 14, pp. 4424–4428, Nov. 2019, https://doi.org/10.1016/j.jeurceramsoc.2019.06.012

[34] K. Z. Rajab *et al*., “Broadband Dielectric Characterization of Aluminum Oxide (Al2O3),” in *Journal of Microelectronics and Electronic Packaging*, vol. 5, no. 1, pp. 2-7, Feb. 2008, https://doi.org/10.4071/1551-4897-5.1.1

[35] M. H. Ullah, M. T. Islam, J. S. Mandeep, and N. Misran, “Design of a Compact Multiband Antenna on Al2O3 Ceramic Material Substrate,” in *Proc. 15th International Conference on Computer and Information Technology (ICCIT)*, Chittagong, Bangladesh, Dec. 2012, https://doi.org/10.1109/ICCITechn.2012.6509765

[36] Jo. Choi, Ja. Choi, and W. Hwang, “Miniature Millimeter-Wave 5G Antenna Fabricated Using Anodized Aluminum Oxide for Mobile Devices,” in *ACS Omega*, vol. 5, no. 40, pp. 26206−26210, Oct. 2020, https://doi.org/10.1021/acsomega.0c03795

[37] K. Xia, H-F. Zhang, “Application of Al2O3 ceramic for a circularly polarized filtering antenna,” in *Alexandria Engineering Journal*, vol. 96, pp. 237–248, Jun. 2024, https://doi.org/10.1016/j.aej.2024.04.014

[38] E. Kepros, Y. Chu, B. Avireni, S. K. Ghosh, B. Wright, and P. Chahal, “Additive Manufacturing of a mmWave Microstrip Leaky Wave Antenna on Thin Alumina Substrate,” in *Proc. IEEE 74th Electronic Components and Technology Conference (ECTC)*, Denver, CO, USA, May 2024, https://doi.org/10.1109/ECTC51529.2024.00289

[39] A.Z. Elsherbeni, P. Nayeri, and C. J. Reddy, *Antenna Analysis and Design Using FEKO*; SciTech Publishing, Edison, NJ, USA, 2014.

[40] T-Y. Shih, and N. Behdad, “Applications of the characteristic mode theory to antenna design,” In *Developments in Antenna Analysis and Design*; Vol. 1, Mittra R., Eds; The Institution of Engineering and Technology: London, United Kingdom, 2019, pp. 1-34.

[41] Y. Yashchyshyn and P. Tokarsky, “Using a Metasurface to Enhance the Radiation Efficiency of Subterahertz Antennas Printed on Thick Substrates,” in *Sci. Rep*., vol. 14, 18167, Aug. 2024, https://doi.org/10.1038/s41598-024-69296-5